

Analysis of a cellulose cross-linking treatment of linen fabric using thermogravimetry

R.D. McCall^{a,*}, H.S.S. Sharma^a, K. Kernaghan^b

^a Applied Plant Science Division, Agri-Food and Biosciences Institute, Newforge Lane, Belfast, BT9 5PX, Northern Ireland, UK

^b Department of Applied Plant Science, School of Agriculture and Food Science, Queens University of Belfast, BT9 5PX, Northern Ireland, UK

Received 14 June 2006; received in revised form 26 March 2007; accepted 1 May 2007
Available online 6 May 2007

Abstract

Reagents may improve crease recovery (CR) in fabrics woven from cellulosic fibres by forming cross-links between cellulose chains. For linen improvements in CR performance are accompanied by a decline in resistance to abrasion (AR) producing a detrimental effect on competitiveness. Conventional measurements of CR and AR are inefficient, require controlled environment and provide no chemical or structural information on the effect or efficiency of the treatments. Thermogravimetric analysis was performed on linen samples treated with a cross-linking agent (DMU). Multivariate analysis was used to establish calibration models relating discrete and continuous data to the required parameters. These models were then validated by prediction. It was demonstrated that the analysis was able to detect the DMU and predict the CR and AR parameters. The best equations were obtained using a heating rate of $20\text{ }^{\circ}\text{C min}^{-1}$ and modelling using continuous data rather than the discrete measurements.

© 2007 Elsevier B.V. All rights reserved.

Keywords: Thermal analysis; Linen; Crease recovery; Chemometrics

1. Introduction

The poor crease recovery performance of linen fabrics has resulted in attempts to improve this characteristic by modifying the structure of the flax fibres from which the linen is woven. One approach has been to cross-link the cellulose polymer chains, cellulose being approximately 75% of the total components of flax fibres [1]. Dimethylolurea (DMU) can achieve this cross-linking by condensation reactions with OH groups on adjacent cellulose chains [2]. The processing technique is capable of producing good improvements in the crease recovery performance in linen, however the treatment has the effect of significantly reducing the fabrics' resistance to abrasion [3]. The conventional physical techniques required to determine crease recovery angle (CR) [4] and abrasion resistance (AR) [5] for fabrics are slow, provide no indication of structural changes or efficiency of the treatment at a molecular level and require environmental control.

The technique of thermogravimetric analysis (TG), and combusting the samples in air, has been demonstrated in Refs. [6,7] to successfully predict flax fibre parameters, such as quality in relation to yarn production and flax fibre fineness. For a flax sample, the derivative of a thermogram displays two active regions of high rate of weight loss at $200\text{--}400\text{ }^{\circ}\text{C}$ and $400\text{--}600\text{ }^{\circ}\text{C}$. The effects in these regions are referred to as peaks 1 and 2, respectively.

The main components of flax fibres are cellulose, hemicelluloses, pectins and lignins [1]. These components have been stated to combust individually in particular temperature ranges, pectin at $200\text{--}290\text{ }^{\circ}\text{C}$, hemicellulose at $243\text{--}305\text{ }^{\circ}\text{C}$, alpha cellulose at $240\text{--}360\text{ }^{\circ}\text{C}$, and straw lignin at $410\text{--}600\text{ }^{\circ}\text{C}$ [8]. Peak 1 can be interpreted as being primarily from a cellulose origin whilst peak 2 is regarded as being caused mainly by combustion of secondary products from the combustion associated with peak 1 along with any contribution from other fractions, such as lignin, rather than combustion of these fractions alone [9].

Previously reported observations in Refs. [7,10] on flax fibres have demonstrated that changes occurring in the combustion peaks such as their temperatures, widths, areas and heights can be related to physical and quality aspects of the fibres.

* Corresponding author. Tel.: +44 28 90255243; fax: +44 28 90255007.
E-mail address: David.Mccall@afbini.gov.uk (R.D. McCall).

Differences in the thermograms have also been reported in Ref. [11] in relation to the heating rate employed and the technique used to prepare samples, with the suggestion that improved resolution might be expected at lower heating rates.

The aims of this study were to investigate thermal characteristics of fabrics treated with different concentrations of DMU and to develop calibration models for predicting crease recovery, abrasion resistance and nitrogen content of fabric.

2. Experimental

2.1. The fabrics

The fabrics used were plain weave linens [12] with a weight of approximately 127 g cm^{-2} . Three rolls of fabric each of approximately 1.5 m width by 50 m length formed the stock materials. The three rolls differing only in their pre-treatment that is one roll each of scoured (S) linen [13], bleached (B) linen [13] and mercerised (M) linen [14]. These pre-treatment covered the commercially available forms of linen fabric.

Samples from the stock fabrics were carefully ruled out following single warp and weft yarns to $21.6 \text{ cm} \times 30.5 \text{ cm}$ for S and B linens, and $23.6 \text{ cm} \times 30.5 \text{ cm}$ for the M linen. The different dimensions for the latter were required to accommodate the approximately 8.5% weft shrinkage associated with mercerised fabric in accordance with commercial practice [14]. The dimensions of the samples were selected to fit pin frames which allowed the drying of the treated samples under constant tension. Two fabric sample sets were prepared. Set 1 consisted of samples S, M, and B linens each treated with 5% dimethylolurea, 2.5% DMU and water as a control [15]. Set 2 consisted of just B linen but treated with water, 2, 4, 7 and 10% DMU. Four replicates fabric sample sheets were prepared for each linen type and treatment for both sets.

2.2. Fabric treatment

Samples were treated with dimethylolurea (Sigma, Poole, Dorset) catalysed with 25% magnesium chloride hexahydrate (Sigma, Poole, Dorset) on weight of DMU selected to optimise formation of cross-links [3], and finally a distilled water control. The solutions were applied by laboratory scale padding mangle (Ernst Benz AG, Zurich), weighed for uptake and dried (approx. 35°C for at least 20 min), before being cured in an oven at $140\text{--}145^\circ\text{C}$ for 4 min. All samples were subsequently after-washed at 60°C for 5 min, using an aqueous solution of 5 g L^{-1} sodium carbonate decahydrate and 0.4 g L^{-1} sodium dodecyl sulphate, in order to remove any unreacted DMU and catalyst, then rinsed in running water for about 10 min. The water treated controls were also washed in this way for consistency. All samples were finally dried on pin frames prior to storing, for a minimum of 2 weeks, at 65% RH and 20°C until required for testing [15].

2.3. Physical assessment

CR angles were determined according to British Standard method [4] under standard conditions. Twelve replicates from

each of the three treatments and from each of the three fabrics, (total sample set $n = 108$), were measured using a crease recovery angle meter (Shirley combined creasing and stiffness tester, Shirley Developments Ltd., Didsbury, UK). The CR angles obtained were recorded as a percentage of 180° , and mean values determined. AR was determined under standard conditions (20°C and 65% humidity), using a Martindale wear and abrasion tester, (J. H. Heal Co., Halifax, UK), with 12 kPa pressure. Four replicates could be accommodated for each abrasion run on this instrument, and the end point was determined by periodic visual inspection of the fabric surface for the first yarn breakage. Each sample was tested using 12 replicates and the mean number of rubs per treatment was calculated [5].

2.4. Elemental analysis

The fabric samples were analysed for percentage nitrogen (N) by pyrolysis gas chromatography. The samples were finely cut using a pair of serrated scissors, and between 5 and 10 mg of each sample, were carefully weighed in tin foil capsules, then enclosed by folding over the tin foil [15]. The capsule pellets were then loaded into the auto-sampler carousel of an elemental analyser (Carlo Erba NA 1500 Series 2, Milan, Italy). The resultant gases such as nitrogen dioxide were measured as percentage nitrogen (N). Each sample was analysed in triplicate [15].

2.5. Thermogravimetric analysis

Sub-samples were cut from the fabric sample sheets and cut finely, using serrated scissors, to give fibre lengths of the order of about 0.1 mm or less [11]. The finely cut sub-samples were stored in labelled sealed petri dishes until required for testing. Three replicates of each cut sub-sample and each treatment were weighed out, in alumina crucibles, on a Metler MT5 six decimal place balance (Metler-Toledo, Switzerland). A weight range of between 3.0 and 3.2 mg was used [11], and the weights recorded to an accuracy of micrograms. The crucibles were then loaded onto the auto-sampler carousel of a Metler Toledo Thermogravimetric Analysis System TGA/SDTA851. The samples were run from 30 to 600°C using a heating rate of $20^\circ\text{C min}^{-1}$ using air as a purge gas [11]. A sample set was also run at a heating rate of 5°C min^{-1} in order to determine improvements in resolution.

2.6. Data analysis

Data obtained from the thermogravimetric runs was analysed in two different ways. Firstly the thermograms obtained were differentiated (DTG) using the Metler Toledo software and the following discrete parameters were measured: peak decomposition temperature, peak area, peak width, residue and weight loss in two decomposition segments $200\text{--}400^\circ\text{C}$ and $400\text{--}600^\circ\text{C}$. The second approach was to export the continuous weight loss data (1704 variables for $20^\circ\text{C min}^{-1}$ and 6819 variables for 5°C min^{-1} heating rates) into Unscrambler V9.1, (CAMO, Trondheim, Norway) for principal component analysis (PCA) and partial least squares (PLS) regression.

PCA of the data was performed to identify any anomalous TG responses, possibly produced as a result of contamination of a specimen or unsatisfactory instrumental response.

The relationships between the calibration set thermal data (discrete and continuous) and measured CR, AR and N values were then investigated using PLS 1 regression. The continuous TG data was first transformed by Savitsky–Golay differentiation using two mathematical treatments (MT) for each heating rate. These were 1st and 2nd order differentiation, smoothing and polynomial order. For example MT = 1442 implies 1st order derivative with smoothing of four points left and four points right and polynomial order 2. Levels of smoothing were chosen to reduce noise.

The relationships developed from these calibration sets were then used to predict CR, AR and N for the validation set. This allowed the performance of the calibration models to be assessed, within the confines of our sample sets.

3. Results

The measured CR, AR and N content are presented in [Table 1a](#) for fabric set 1 (calibration set) and in [Table 1b](#) for fabric set 2 (validation set). [Table 1a](#) illustrates the fixation of nitrogen from

Table 1

(a) The effects of DMU treatment on bleached, scoured and mercerised fabric samples for changes in crease recovery (CR), abrasion resistance (AR), and nitrogen content (N) of samples from the calibration set (set 1) [15] and (b) the effects of DMU treatment on bleached, samples validation set (set 2)

(a) Treatment	Bleached	Scoured	Mercerised		
CR (%)					
Control	25.5	22.4	20.8		
2.5% DMU	49.2	44.4	35.1		
5% DMU	60.8	58.3	51.9		
S.E.M.s; fabric = 0.557*** DMU = 0.557*** fabric × DMU = 0.966***					
AR (rubs)					
Control	6135	7838	18444		
2.5% DMU	3712	10292	23393		
5% DMU	600	1471	10402		
S.E.M.s; fabric = 144.3*** DMU = 144.3*** fabric × DMU = 790.6***					
N (%)					
Control	0.008	0.056	0.033		
2.5% DMU	0.562	0.595	0.557		
5% DMU	1.224	1.2467	1.1273		
S.E.M.s; fabric = 0.005*** DMU = 0.005*** fabric × DMU = 0.009***					
(b) Treatment	Water control	2% DMU	4% DMU	7% DMU	10% DMU
CR (%)					
Control	23.79	36.11	53.26	60.36	54.48
S.E.M.s	0.918	0.522	0.831	0.828	1.031
AR (rubs)					
Control	6675	7575	1600	975	650
S.E.M.s	295	882	167	138	119
Nitrogen (%)					
Control	<0.1	0.430	1.267	1.867	2.610
S.E.M.s		0.015	0.013	0.053	0.085

S.E.M.s—standard error of means.

*** $P < 0.001$.

the DMU treatment in the fabric. Increasing the concentration of DMU in the treatment resulted in an increase in stabilised nitrogen in the three types of fabric ([Table 1a](#)). Similarly for CR ([Table 1a](#)), increasing the concentration of DMU in the treatment resulted in an improvement increase recovery angle, measured as a percentage of 180°, for the three fabrics. AR displays a more anomalous behaviour ([Table 1a](#)). Treatment of the S and M fabrics with 2.5% DMU produced an improvement in AR, whilst the B fabric exhibited a reduction in AR. It was also observed that the M linen gives by far the best AR performance in comparison with the B and S fabrics. Sample set 2 ([Table 1b](#)) exhibited the same effects as the B fabrics of set 1.

Three thermogravimetric analysis runs were performed on each fabric at each DMU concentration and also at each of the two heating rates. The averaged DTG plots for the B fabrics at heating rates of 20 °C min⁻¹ ([Fig. 1a](#)) and 5 °C min⁻¹ ([Fig. 1b](#)) are presented. The thermograms illustrated the two-step combustion in air of flax fibre and the DTG plots are presented for clarity. Step one of the thermograms is from 200 to 400 °C and corresponds to the peak 1 region of the 1st derivative. The second TG step occurs between 400 and 600 °C, and corresponding to the peak 2 region of the 1st derivative ([Fig. 1](#)). These steps are caused by the samples losing weight in response to heating. No differences were observed between the S, M and B linens at any one treatment hence, for clarity, only the B fabrics are presented. However, within each DMU treatment set the thermograms revealed clear differences. The 0% DMU or water treated control presents a single DTG peak 1 occurring at 354 °C on the 20 °C min⁻¹ plot and 325 °C on the 5 °C min⁻¹ plot. As the percentage of DMU in the treatment increases DTG peak 1 appeared to expand towards higher temperatures by a new peak appearing at the higher temperatures (359 °C at the high and 331 °C low rates of heating). The peak 1 height or the maximum rate of weight loss decreases with increasing DMU application. The maximum rate of weight loss associated with peak 2 remained fairly constant but expanded towards the higher temperature with increasing concentration of DMU.

The descriptive statistics for the complete sample sets, one set at 20 °C min⁻¹ heating rate, and one set at 5 °C min⁻¹ heating rate, are presented in [Table 2](#). Measurements were taken of the 11 parameters and revealed a range, mean and standard deviation of the readings for each parameter for each of the two heating rates used and the differences between the two heating rates ([Table 2](#)). Distinctive changes for sample set 1 ([Table 2a](#) and [b](#)) are summarized below.

The maximum rate of weight loss in peak 1 (P1-h) is reduced from 1.26 to 0.29 mg min⁻¹ for the 5 °C min⁻¹ heating rate and the mean peak 1 temperature (P1-t) is reduced from 356.9 to 321.0 °C. Similarly the maximum rate of weight loss in peak 2 (P2-h) fell from 0.28 to 0.044 mg min⁻¹ and the mean peak 2 temperature (P2-t) is reduced from 491.0 to 459.8 °C for the low heating rate. Similar trends can be clearly seen in the set 2 validation samples ([Table 2c](#) and [d](#)).

The statistical results obtained in developing the calibration models (sample set 1 only) are presented in [Table 3](#). The SEC

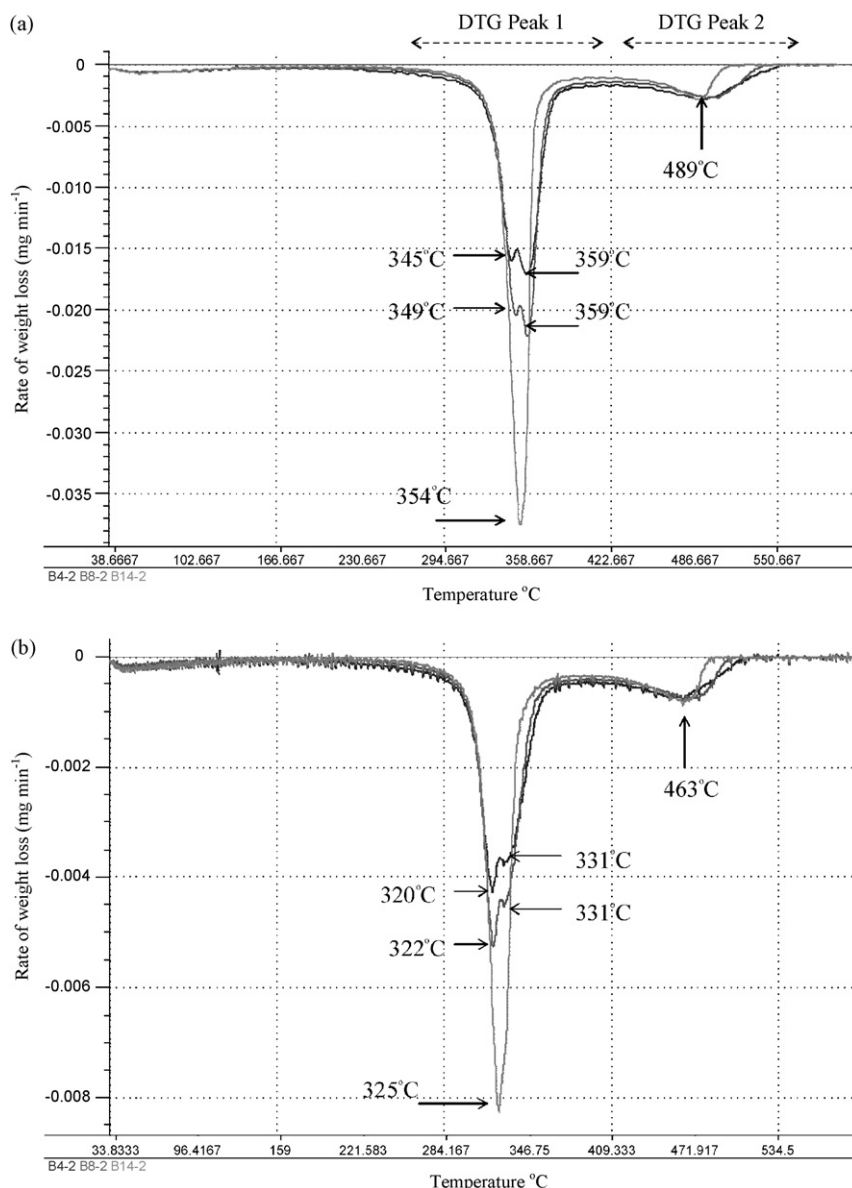


Fig. 1. Overlays of derivative thermograms from bleached linen treated with water (light grey), 2.5% DMU (grey) and 5% DMU (black) combusted at and (a) 20°C and (b) 5°C heating rates.

values are the standard errors in the calibration, and the R^2 calibration values are the correlation between the X variable sets and the Y variable sets. Once the calibration had been established then one sample could be removed and the calibration modified. The removed sample was then compared with the modified calibration. This was repeated for all samples, giving the cross validation values, SECV being the standard error in the cross validation, and the R^2 validation value is the correlation determined in the cross validation procedure.

For the $5^{\circ}\text{C min}^{-1}$ (Table 3a) SEC and related R^2 calibration values, the continuous data appears to out perform the discrete data notably in reducing SEC values by a factor of about 2. Nitrogen content data revealed an exception to this appearing to calibrate with similar SEC values for discrete, 1st and 2nd derivative data. The best AR figure of 845.7 rubs was obtained using the continuous data set and the 2nd derivative mathemat-

ical treatment (2862), whilst best SEC value for CR of 1.88% was obtained using the 1st derivative mathematical treatment (1442). Cross validation of this calibration produced the typical increase in SECV with respect to SEC for the discrete data and the continuous 1442 data, and reductions in the R^2 for cross validation values. However, the 2nd derivative (2862) performance for AR, CR and N revealed large increases in SECV values, most noticeable for AR with respect to SEC values. Also noted was the reduction in R^2 for cross validation, particularly for AR which showed a drop from R^2 calibration value of 0.99 to R^2 cross validation of 0.63.

The calibration performance for the $20^{\circ}\text{C min}^{-1}$ heating rate is presented in Table 3b and shows a similar pattern to the $5^{\circ}\text{C min}^{-1}$ data with the exception of the second differential (MT = 2862) for AR, CR and N. No large fluctuations in cross validation performance, as noted above, were observed.

Table 2

Discrete thermal statistics for calibration (a and b) and validation (c and d) sets, one set run at 5 °C min⁻¹ and the other at 20 °C min⁻¹ showing minimum, maximum, mean and standard deviations (S.D.) for peak 1 area (P1-a, %), peak 1 height (P1-h, mg min⁻¹), peak 1 width (P1-w, °C), peak 2 area (P2-a, %), peak 2 height (P2-h, mg min⁻¹), peak 2 width (P2-w, °C), weight loss in peak 1 (WL1, %) and weight loss in peak 2 (WL2, %)

	P1-a	P1-h	P1-t	P1-w	P2-a	P2-h	P2-t	P2-w	WL1	WL2	Residue
(a) 20 °C heating rate											
Minimum	50.12	0.75	345.3	20.1	7.46	0.12	475.3	5.4	70.94	14.58	3.53
Maximum	70.46	2.21	361.1	40.2	12.91	0.87	504.3	58.8	82.15	25.96	8.86
Mean	58.16	1.26	356.9	30.5	11.11	0.28	491.0	37.1	75.68	21.11	4.32
S.D.	6.62	0.49	4.1	7.2	1.43	0.27	9.2	18.7	3.54	3.74	1.24
(b) 5 °C heating rate											
Minimum	48.68	0.18	317.5	18.6	10.34	0.032	450.8	29.1	73.59	17.16	2.68
Maximum	65.02	0.48	324.1	40.2	12.83	0.056	472.0	56.2	79.97	22.67	9.28
Mean	56.34	0.29	321.0	30.2	11.81	0.044	459.8	41.2	76.18	20.26	4.36
S.D.	4.84	0.09	2.2	7.1	0.57	0.008	5.8	8.4	1.88	1.80	1.25
(c) 20 °C heating rate											
Minimum	51.10	0.79	353.7	19.8	8.23	0.120	487.8	29.2	71.99	14.46	2.01
Maximum	69.65	2.22	361.3	37.9	11.77	0.160	504.9	59.8	83.73	24.03	6.53
Mean	58.53	1.29	358.0	30.2	10.62	0.128	496.2	49.5	75.72	20.46	2.87
S.D.	6.73	0.54	2.4	7.0	1.27	0.014	6.6	10.3	3.89	3.46	1.43
(d) 5 °C heating rate											
Minimum	52.79	0.20	319.3	18.4	10.48	0.031	460.1	36.0	74.53	17.11	2.42
Maximum	67.69	0.49	325.1	36.5	11.94	0.044	472.7	51.8	82.34	21.26	10.84
Mean	58.29	0.30	321.7	29.7	11.26	0.036	465.4	46.4	76.95	19.86	3.58
S.D.	5.30	0.11	2.3	6.9	0.46	0.004	5.7	5.8	2.19	1.49	2.03

However, it must be noted that model 18 did generate a high SEC value. In general, for the development of calibration models, the 5 °C min⁻¹ heating rate produced the lowest calibration errors and highest correlations with 1st derivative continuous data appearing to perform better than the discrete data. A 2nd derivative 5 °C min⁻¹ heating rate showed some early indications of model instability, such as relatively large differences

between SEC and SECV values and between their corresponding R^2 results.

The calibration models were then validated by predicting AR, CR and N performances of set 2 fabrics. Table 4 lists the standard error in prediction (SEP) with their associated correlation (R^2), slope and bias of the graphs of predicted against measured values for AR, CR and N and for each calibration model. The

Table 3

Comparison of calibration equations developed from discrete data (DD) and continuous (CD) weight loss data (MT = mathematical treatment, SEC = standard error in calibration, SECV = standard error in cross validation)

Model no.	Data type	MT	Parameter	SEC	R^2 calibration	SECV	R^2 validation
(a) 5 °C/min heating rate							
1	DD	None	AR	3177.6	0.88	4113.3	0.79
2		None	CR	3.49	0.97	4.25	0.96
3		None	N	0.05	0.99	0.06	0.99
4	CD	1442	AR	1428.2	0.98	2060.0	0.95
5		1442	CR	1.88	0.99	2.63	0.98
6		1442	N	0.06	0.99	0.08	0.99
7	CD	2862	AR	845.7	0.99	5968.8	0.63
8		2862	CR	1.93	0.99	5.77	0.94
9		2862	N	0.06	0.99	0.20	0.92
(b) 20 °C/min heating rate							
10	DD	None	AR	4249.6	0.82	6362.4	0.57
11		None	CR	6.53	0.90	7.07	0.88
12		None	N	0.17	0.93	0.19	0.92
13	CD	1442	AR	2109.5	0.95	3197.7	0.88
14		1442	CR	3.20	0.98	4.19	0.96
15		1442	N	0.08	0.99	0.09	0.98
16	CD	2862	AR	2367.9	0.93	3501.2	0.85
17		2862	CR	2.76	0.98	3.66	0.97
18		2862	N	0.77	0.99	0.09	0.98

Table 4
Validation of the calibration models listed in Table 3 using an independent set of 15 samples (U = unstable, SEP = standard error in prediction)

Model no.	Parameter	SEP	R^2	Slope	Bias
1	AR	4250.6	0.80	1.61	-2132.2
2	CR	3.14	0.98	0.89	0.61
3	N	0.61	0.90	0.40	-0.572
4	AR	6540.9	0.818	2.32	-2446.6
5	CR	6.61	0.915	1.06	4.19
6	N	0.48	0.935	0.55	-0.43
7	AR	3629.8	0.294	0.28	3209.7
8	CR	6.49	0.95	0.58	-1.74
9	N	0.74	0.843	0.25	-0.53
10	AR	U	U	U	U
11	CR	8.90	0.96	0.38	-6.06
12	N	0.81	0.81	0.16	-.62
13	AR	4897.2	0.82	1.86	-1553.7
14	CR	2.55	0.986	1.04	2.95
15	N	0.52	0.930	0.51	-0.45
16	AR	1568.1	0.864	0.78	-907.4
17	CR	2.60	0.983	0.96	1.84
18	N	0.52	0.936	0.49	-0.52

performance of the models were assessed according to which predicted AR, CR and N with the lowest SEP, highest R^2 , slope closest to 1 and bias closest to 0, in order of priority.

AR was found to be predicted best by model 16, which was developed from the 2nd derivative of the continuous thermal data. These were $20\text{ }^\circ\text{C min}^{-1}$ heating rate and produced values for SEP = 1568.1 rubs, $R^2 = 0.86$, slope = 0.78 and a bias of 907.4 rubs. CR angle was found to be predicted best by model 14 which, in this case, was developed from a 1st derivative of the continuous thermal data. These were at the $20\text{ }^\circ\text{C min}^{-1}$ heating rate showing a SEP = 2.55%, $R^2 = 0.986$, slope = 1.04 and a bias of 2.95%. In addition, a good CR performance was obtained from model number 17, with the 2nd derivative mathematical treatment at a heating rate of $20\text{ }^\circ\text{C min}^{-1}$. Nitrogen content was found to be predicted best by model 6 which was developed from a 1st derivative of the continuous data at the $5\text{ }^\circ\text{C min}^{-1}$ heating rate. The measured SEP, R^2 , slope and bias were 0.48%, 0.935, 0.55 and -0.43%, respectively. The best performing models performance in prediction are presented in Fig. 2 as predicted versus measured plots. The AR plot reveals a probable error by producing a negative prediction (lower than -2000 cycles) for one replicates. Eliminating this replicate as a probable outlier improved the prediction statistics ($R^2 = 0.898$ and SEP = 1428.3). However, for completeness the replicate has been left included in the result given in Table 4.

4. Discussion

The results of these studies have shown that the thermal technique is capable of revealing the effect of DMU treatment visually in a thermogram. DMU is capable of forming cross-links between adjacent cellulose chains by reacting with available OH groups [15]. Observations of the 1st derivatives of the thermograms reveal increasing widths of peaks 1 and 2 towards higher temperatures and reducing peak 1 heights with

increased concentration of DMU. The appearance of new peaks only in the plots of DMU treated samples, at $359\text{ }^\circ\text{C}$ in the higher heating rate and $331\text{ }^\circ\text{C}$ in the lower heating rate trials (Fig. 1) can only be caused by the DMU incorporated in the fabric. This suggests that the new peak is related to, or directly caused by, cross-linked cellulose that may undergo combustion at a higher temperature than cellulose that is not cross-linked. This hypothesis, if correct, may indicate a means of determining the degree of actual cross-linkage taking place.

Fabric parameters, such as CR angle measurement and AR determination, are essential tests required to measure the performance of a CR treatment. They are time consuming tests requiring conditioned environments and samples, but can give useful reproducible results and the lowest standard error performance (Table 1a and b). Any instrumental analysis technique attempting to relate to these performance parameters must also address the inherent performance error relative to the physical tests. The performance error of any instrumental technique is unlikely to be as low as the physical test it is intended to replace [16]. Hence, the error generated in the instrumental analysis must be minimised to achieve a value as close as possible to the error achieved in the physical testing.

The thermal technique has been demonstrated as being able to predict CR and AR. By careful choice of heating rate and optimised modelling technique thermal analysis can perform well (Table 4). The best results were obtained from the $20\text{ }^\circ\text{C min}^{-1}$ heating rate, which was a surprising result. The lower heating rate, with much greater number of data points in a thermogram, should result in better resolution hence better modelling and predictive performance. Although this appeared to be occurring at the development of calibration equations, this apparent improvement did not occur at the validation stage.

The chemometric modelling for CR, AR and N clearly demonstrated that the application of the continuous data for modelling outperforms modelling with discrete data. Also the choice of using 1st or 2nd derivative transformation is important, notably for AR determination which provided the best results using 2nd derivative at the higher heating rate. At the lower heating rate 2nd derivative results became unstable, possibly caused by cumulative noise. The low heating rate thermograms are noisier than those obtained at the higher heating rate and this noise will increase at each differentiation. The calibration equations were examined for key variables contributing to accuracy/stability of the models. In the case of discrete variables the regression coefficients for P1-t, P2-a, P2-h, P2-w and residue were significantly higher than the other six parameters.

SEPs using the DTG data are however much higher than the standard errors generated using the physical tests. The SEP performance should improve markedly using a much larger data set, however the instrumental technique may indicate higher errors than the direct physical measurement. Nevertheless, the instrumental technique has an advantage of delivering additional structural and or chemical information.

Thermal analysis is a rapid process relative to conventional physical CR and AR determination techniques and can be configured to allow continuous unattended operation. TG is a technique that would not be suitable for 'in line' application. However and

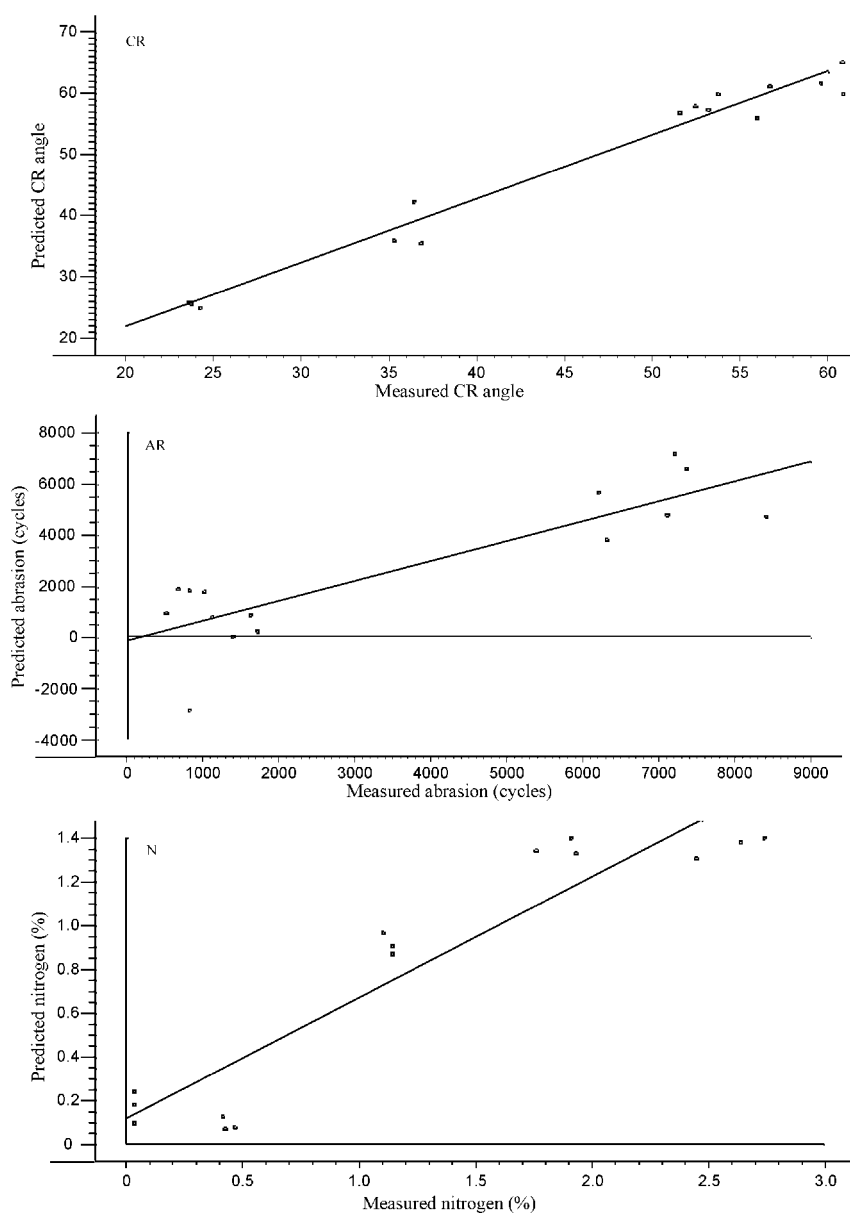


Fig. 2. Predicted vs. measured validation plots of best predicting models (Table 4) for crease recovery angle using model 14 (CR), abrasion resistance in Martindale cycles using model 16 (AR) and % nitrogen content using model 6 (N).

perhaps importantly, when considering possible global application, thermal analysis has no requirement for conditioning of samples or environment.

The equipment cost of setting up and maintaining thermal systems are considerably higher than the physical measurement systems, and the requirements of a higher technical skill level are the main disadvantages. Also it may be necessary to recalibrate to suit different fabric types, since these particular models have been developed using only one fabric weight of plain weave un-dyed linen.

References

- [1] B. Focher, A. Marzetti, H.S.S. Sharma, in: H.S.S. Sharma, C. Van Sumere (Eds.), *The Biology and Processing of Flax*, M Publications, Belfast, 1992, pp. 329–342.
- [2] F.R.W. Sloan, *J. Soc. Dyers Colour.* 113 (1997) 46.
- [3] S.A. Heap, R.E. Hunt, P.A. Rennison, R. Tattersall, in: H. Mark, N.S. Wooding, S.M. Atlas (Eds.), *Chemical After Treatment of Textiles*, Wiley, New York, 1971, pp. 267–317.
- [4] Anon, British Standards Institution, London, 1972, pp. 35–39 sec 4.
- [5] Anon, *Method of Test for Determination of the Abrasion Resistance of Fabrics*, British Standards Institution, London, 1979, BS5690.
- [6] H.S.S. Sharma, K. Kernaghan, *Thermochim. Acta* 132 (1988) 101–109.
- [7] G. Faughey, H.S.S. Sharma, R.D. McCall, *J. Appl. Polym. Sci.* 75 (2000) 508–514.
- [8] H.S.S. Sharma, *Thermochim. Acta* 285 (1996) 211–220.
- [9] T. Fisher, M. Hajaligol, B. Waymac, D. Kellogg, *J. Anal. Appl. Pyrolysis* 62 (2002) 331–349.
- [10] H.S.S. Sharma, D. McCall, K.J. Kernaghan, *J. Appl. Polym. Sci.* 72 (1999) 1209–1219.
- [11] H.S.S. Sharma, G. Faughey, D. McCall, *J. Textile Inst.* 87 (2) (1996) 249–257 (part 1).

- [12] L. Vangheluwe, P. Kiekens, in: H.S.S. Sharma, C. Van Sumere (Eds.), *The Biology and Processing of Flax*, M Publications, Belfast, 1992, pp. 447–461.
- [13] K. Kernaghan, P. Kiekens, in: H.S.S. Sharma, C. Van Sumere (Eds.), *The Biology and Processing of Flax*, M Publications, Belfast, 1992, pp. 343–445.
- [14] K. Kernaghan, in: H.S.S. Sharma, C. Van Sumere (Eds.), *The Biology and Processing of Flax*, M Publications, Belfast, 1992, pp. 475–500.
- [15] R.D. McCall, K.J. Kernaghan, H.S.S. Sharma, *J. Appl. Polym. Sci.* 82 (2001) 1886–1896.
- [16] F.E. Barton II, in: G.C. Marten, J.S. Shenk, F.E. Barton II (Eds.), *Near Infrared Reflectance Spectroscopy (NIRS): Analysis of Forage Quality*, USDA, Agricultural Research Service, Agriculture Handbook No. 643, Springfield, USA, 1989, p. 68.